Bi-transgenic Mice Reveal that K-ras^{Val12} Augments a p53-independent Apoptosis When Small Intestinal Villus Enterocytes Reenter the Cell Cycle

Craig M. Coopersmith,[*][‡] Chitra Chandrasekaran,[*] M. Shane McNevin,[*][‡] and Jeffrey I. Gordon[*]

[*]Department of Molecular Biology and Pharmacology, [‡]Department of Surgery, Washington University School of Medicine, St. Louis, Missouri 63110

Abstract. Studies in cell culture systems have indicated that oncogenic forms of Ras can affect apoptosis. Activating mutations of Ras occur in ~30% of all human tumors and 50% of colorectal carcinomas. Since these mutations appear at early or intermediate stages in multistep journeys to neoplasia, an effect on apoptosis may help determine whether initiated cells progress towards a more neoplastic state. We have tested the effects of K-ras^{Val12} on apoptosis in transgenic mice. A lineage-specific promoter was used to direct expression of human K-ras^{Val12}, with or without wild-type (wt) or mutant SV-40 T antigens (TAg), in postmitotic villus enterocytes, the principal cell type of the small intestinal epithelium. Enterocytes can be induced to reenter the cell cycle by TAg^{Wt}. Reentry is dependent upon the ability of TAg to bind pRB and is associated with a p53-independent apoptosis. Analyses of K-ras^{Val12} × TAg^{Wt} bi-transgenic animals indicated that K-ras^{Val12} can enhance this apoptosis threefold but only in cycling cells; increased apoptosis does not occur when K-ras^{Val12} is expressed alone or with a TAg containing Glu^{107,108}→Lys^{107,108} substitutions that block its ability to bind pRB. Analysis of bi-transgenic K-ras^{Val12} × TAg^{Wt} mice homozygous for wild-type or null p53 alleles established that the enhancement of apoptosis occurs through a p53-independent mechanism, is not attributable to augmented proliferation or to an increase in abortive cell cycle reentry (compared to TAg^{Wt} mice), and is not associated with detectable changes in the crypt–villus patterns of expression of apoptotic regulators (Bcl-2, Bcl-x$_L$, Bak, and Bax) or mediators of epithelial cell–matrix interactions and survival (e.g., $\alpha_5\beta_1$ integrin and its ligand, fibronectin). Coexpression of K-ras^{Val12} and TAg^{Wt} produces dysplasia. The K-ras^{Val12}-augmented apoptosis is unrelated to this dysplasia; enhanced apoptosis is also observed in cycling nondysplastic enterocytes that produce K-ras^{Val12} and a TAg with a COOH-terminal truncation. The dysplastic epithelium of K-ras^{Val12} × TAg^{Wt} mice does not develop neoplasms. Our results are consistent with this finding: (*a*) When expressed in initiated enterocytes with a proliferative abnormality, K-ras^{Val12} facilitates progression to a dysplastic phenotype; (*b*) by diminishing cell survival on the villus, the oncoprotein may impede further progression; and (*c*) additional mutations may be needed to suppress this proapoptotic response to K-ras^{Val12}.

A CTIVATING mutations of Ras genes are encountered in ~30% of all human tumors and in 50% of colorectal carcinomas (Bos et al., 1987; Forrester et al., 1987; Fearon and Vogelstein, 1990). These mutations have been generally described as early or intermediate events in multistep journeys to neoplasia (Barbacid, 1987; Fearon and Vogelstein, 1990). Studies of cultured cells have shown that oncogenic forms of Ras can provoke premature senescence or influence apoptosis—two responses that can have an important impact on tumorigenesis.

Serrano et al. (1997) found that expression of an oncogenic form of Ras in primary cultures of human and rodent cells produces premature senescence, with permanent arrest in G1. This effect is associated with an induction of p53 as well as p16^{INK4a}, the inhibitor of cyclin-dependent kinase (cdk)[1] 4 and cdk6. The association is causal rather than casual: inactivation of either p53 or p16 suppresses the senescence response to oncogenic Ras. The implications of this finding to the origins of neoplasia are

1. *Abbreviations used in this paper*: BrdU; 5-bromo-2′-deoxyuridine; cdk, cyclin-dependent kinase; Cy3, indocarbocyanine; *Fabpi*, intestinal fatty acid–binding protein gene; FITC, fluorescein isothiocyanate; P, postnatal day; SV-40 TAg, simian virus 40 large T antigen; TUNEL; terminal deoxynucleotidyltransferase (TdT)–mediated, dUTP nick end labeling.

great (Serrano et al., 1997; for review see Weinberg, 1997). p53 and/or p16 mutations are encountered in most human tumors (Hollstein et al., 1994; Hirama and Koeffler, 1995). Senescence can be viewed as a protective, antineoplastic "host" response to an initial activating Ras mutation, a response that can be overridden by subsequent inactivating mutations of either p16 or p53, thereby allowing progression (transformation). This view fits with the multistep model of human colorectal carcinoma, where early mutation of Ras is followed by p53 inactivation (Fearon and Vogelstein, 1990). The findings of Serrano and co-workers also provide a rationale for two well-known phenomena: (*a*) Primary cultures of embryonic cells are resistant to transformation by oncogenic forms of Ras (Newbold and Overell, 1983), while immortalized cells, which have often acquired inactivating p16 or p53 mutations, are very sensitive to transformation. (*b*) Oncogenic forms of Ras cooperate with viral oncoproteins, such as E1A or SV-40 large T antigen (SV-40 TAg), to transform primary cell cultures. Both of these viral proteins bind to and disable pRB, producing an effect functionally analogous to p16 inactivation, since pRB is the principal substrate for phosphorylation by cdk4 and cdk6 (Weinberg, 1995, 1997). In the case of SV-40 TAg, both pRB and p53 are bound and inactivated.

Apoptosis represents another response that initiated cells may marshal to prevent their amplification. Studies of various established cultured cell lines have revealed that oncogenic forms of Ras can affect apoptosis. Promotion as well as suppression of cell death has been reported (Fernandez et al., 1994; Chen and Faller, 1995; Kinoshita et al., 1995; Lin et al., 1995; Rak et al., 1995; Wang et al., 1995). Promotion of apoptosis in initiated cells should impede their progression, while inhibition of apoptosis would be expected to help facilitate tumorigenesis.

The effect of Ras oncoproteins on apoptosis or senescence has not been examined using genetically defined in vivo models. The impact of a lineage's state of differentiation and/or proliferative status on Ras-modulated demise or survival can be assessed in transgenic mice where the activated oncoprotein can be directed to selected target cell populations. The self-renewing small intestinal epithelium of the adult mouse represents an attractive system for conducting such an analysis. Its attractiveness stems from the fact that proliferation, differentiation, and death programs are continuously expressed in spatially well-defined domains of crypt–villus units. Normally, these decisions are precisely coordinated to maintain cellular census. Proliferation is limited to crypts of Lieberkühn. Each crypt contains one or more active multipotent stem cell located near its base (Loeffler et al., 1993). The stem cell gives rise to four principal epithelial cell lineages that complete their terminal differentiation during a highly organized, rapid migration. Postmitotic absorptive enterocytes, mucus-producing goblet cells, and enteroendocrine cells exit the crypt and move up an adjacent villus in vertical coherent columns (Schmidt et al., 1985; Hermiston et al., 1996). Cells are removed from the villus tip by apoptosis and/or extrusion into the lumen (Hall et al., 1994). The entire sequence is completed in 3–5 d (Cheng, 1974*a*; Cheng and Leblond, 1974*a–c*). In contrast, members of the Paneth cell lineage undergo terminal differentiation as they move down to the base of the crypt, where they are subsequently removed after an ~20-d residence (Cheng, 1974*b*). The availability of lineage-specific promoters that function at selected locations along the crypt–villus units (e.g., Cohn et al., 1992; Bry et al., 1994; Simon et al., 1995, 1997) makes it possible to introduce activated Ras oncoproteins in specified cellular contexts and explore their effects on survival or death.

In the present report, we have used transgenic mice to examine the effects of expressing human K-ras^{Val12} in postmitotic villus enterocytes. K-ras^{Val12} was also coexpressed with wild-type or mutant SV-40 TAg's that affect the proliferative status of these cells. The results disclose that K-ras^{Val12} can promote a p53-independent apoptosis that occurs when enterocytes undergo pRB-related reentry into the cell cycle.

Materials and Methods

Production and Maintenance of Transgenic Mice

FVB/N transgenic mice containing nucleotides −1178 to +28 of the rat intestinal fatty acid–binding protein gene (*Fabpi*) linked to human K-ras^{Val12}, wild type (Wt) SV-40 TAg, SV-40 TAg$^{K107/8}$ (mutant 3213 in Chen et al., 1992), or SV-40 TAg$^{\Delta122 \text{ to } 708}$ (mutant dl1137 in Pipas et al., 1983) were generated as described in earlier reports (Kim et al., 1993, 1994; Chandrasekaran et al., 1996). Transgenics were maintained by crosses to normal FVB/N littermates. Male and female C57Bl/6 p53$^{+/+}$ and p53$^{-/-}$ animals were purchased from GenPharm International (Mountain View, CA).

FVB/N *Fabpi*–K-ras^{Val12} transgenic mice were crossed to FVB/N *Fabpi*–SV-40 TAg^{Wt}, *Fabpi*–SV-40 TAg$^{K107/8}$, or *Fabpi*–SV-40 TAg$^{\Delta122 \text{ to } 708}$ animals to generate bi-transgenic mice. Animals were genotyped using tail DNA and PCR protocols detailed elsewhere (Kim et al., 1993, 1994; Chandrasekaran et al., 1996).

FVB/N normal, *Fabpi*–K-ras^{Val12}, *Fabpi*–SV-40 TAg^{Wt}, and *Fabpi*–K-ras^{Val12} × *Fabpi*–SV-40 TAg^{Wt} transgenic mice homozygous for p53 wild-type or null alleles were generated by a series of crosses to C57Bl/6 p53$^{+/+}$ and C57Bl/6 p53$^{-/-}$ animals.

Mice were maintained in microisolator cages under a strict light cycle (lights on at 0600 h and off at 1800 h). Animals were given a standard irradiated chow diet (Pico rodent chow 20; Purina Mills, Inc., St. Louis, MO) ad libitum. Routine screens for Hepatitis, Minute, Lymphocytic Choriomeningitis, Ectromelia, Polyoma, Sendai, Pneumonia, and mouse adenoviruses, enteric bacterial pathogens, and parasites were negative.

Characterization of Transgenic Mice

Western Blots. Animals were sacrificed, and their gastrointestinal tracts were removed en bloc. The small intestine was subdivided into thirds (defined as duodenum, jejunum, and ileum). The distal half of the middle segment ("distal jejunum") was snap frozen in liquid N_2, lyophilized, pulverized, and then resuspended in extraction buffer (50 µg lyophilized tissue/ml buffer; extraction buffer = 40 mM Tris, pH 6.8, 2% 2-mercaptoethanol, 1% SDS, 5% glycerol, 10 mM EDTA, 50 µg/ml aprotinin [Sigma Chemical Co., St. Louis, MO], 50 µg/ml leupeptin [Sigma Chemical Co.], 500 µg/ml Pefabloc [Boehringer Mannheim Corp., Indianapolis, IN], and 10 µg/ml pepstatin A [Sigma Chemical Co.]). Samples were boiled for 5 min, and insoluble debris was removed by centrifugation for 3 min at 12,000 *g*. The protein concentration of the cleared supernatant was determined using the DC Protein Assay kit (BioRad Labs., Hercules, CA). Extracted cellular proteins (75 µg/sample) were fractionated by SDS-PAGE (Laemmli, 1970) and electrophoretically transferred to polyvinylidene difluoride membranes (Amersham Corp., Arlington Heights, IL). Membranes were stained with Ponceau red to verify equivalent transfer of all samples. Blots were pretreated in PBS-blocking buffer (1% gelatin, 0.2% Tween-20 in PBS) for 1 h at 23°C and then incubated in blocking buffer for 2 h at 23°C with: (*a*) affinity purified rabbit anti–Bcl-2 raised against a peptide spanning residues 4–21 of the mouse protein (Santa Cruz Biochemicals, Santa Cruz, CA; final dilution in blocking buffer = 1:500); (*b*) affinity-purified rabbit anti-Bax raised against amino acids 11–30 of the mouse protein (Santa Cruz Biochemicals; 1:500); (*c*) two preparations of affinity-purified antibodies raised in rabbits against a peptide spanning residues 43–61 of

mouse Bax (obtained from Santa Cruz Biochemicals and from Stanley Korsmeyer, Washington University School of Medicine; 1:500); (*d*) affinity-purified rabbit antibodies against a peptide corresponding to amino acids 2–19 of mouse Bcl-x (Santa Cruz Biochemicals; 1:500); (*e*) affinity-purified rabbit antibodies to residues 629–648 of mouse c-Raf-1 (Santa Cruz Biochemicals; 1:500); (*f*) rabbit anti–mouse cdk4 (Santa Cruz Biochemicals; 1:1,000); (*g*) rabbit anti–mouse cdk2 (Santa Cruz Biochemicals; 1:1,000); (*h*) mouse SV-40 TAg mAbs (1:1,000; PharMingen, San Diego, CA); (*i*) rabbit antiactin (Sigma Chemical Co.; 1:5,000); and (*j*) rabbit anti–rat liver fatty acid binding protein (L-Fabp; Sweetser et al., 1988; 1:7,000). Antigen–antibody complexes were visualized with alkaline phosphatase-conjugated secondary antibodies and a chemiluminescent substrate using the Western Light® kit (Tropix, Inc., Bedford, MA). All experiments were performed using three to eight animals/genotype and repeated on two to six occasions.

Blocking controls were performed by preincubating antibodies with a 10-fold weight excess of their corresponding peptide antigens for 1 h at 23°C before probing the blots. In addition, the specificity of the Bax antibody preparations was established by probing Western blots containing proteins extracted from the distal jejunum, spleen, and thymus of mice that were homozygous for wild-type or null alleles of the Bax gene (tissues obtained from S. Korsmeyer; Knudson et al., 1995).

Immunohistochemical Analysis of the Expression of Regulators of the G1/S Transition and of Apoptosis

Postnatal day 42 to 60 (P42–60) male and female FVB/N mice containing one or two transgenes and their normal littermates (*n* = 10 animals/genotype) were given an intraperitoneal injection of 5-bromo-2'deoxyuridine (BrdU; Sigma Chemical Co.; 120 mg/kg body weight) and 5-fluoro-2'-deoxyuridine (Sigma Chemical Co.; 12 mg/kg) 90 min before sacrifice to label cells in S-phase. The small intestine was removed, flushed with PBS, fixed in Bouin's solution for 6–12 h, washed with 70% ethanol, and then divided into proximal and distal halves. Each half was opened with an incision along its cephalocaudal axis and then rolled from its proximal to distal end. Each of the resulting "Swiss rolls" was then cut in half parallel to the duodenal–ileal axis and placed in a tissue cassette with the cut edge of one half facing down and the cut edge of the other half facing up. After embedding in paraffin, serial 5-μm-thick sections were prepared. Alternatively, small intestine was fixed in 10% buffered formalin (Baxter Heathcore Corp., Mundelein, IL) for 4 h and processed as above.

All immunohistochemical manipulations were performed using the MicroProbe system (Fisher Biotech, Chicago, IL). Bouin's- or formalin-fixed sections were deparaffinized in xylene and isopropanol and were then subjected to an antigen unmasking protocol consisting of a 4-min incubation at 37°C in type II bovine pancreas α-chymotrypsin (Sigma Chemical Co.; specific activity = 50 U/mg; final concentration = 1 mg enzyme/ml of 7 mM $CaCl_2$, pH 7.8). The treated sections were washed in PBS, placed in histo-blocking buffer (BSA [1% wt/vol], Triton X-100 [0.3%], powdered skim milk [0.2%] in PBS) for 15 min at 23°C followed by an overnight incubation at 4°C with: (*a*) two different preparations of rabbit anti–mouse Bcl-2; one was the peptide-specific antibody described above (1:50), the other was raised against a glutathione S–transferase fusion protein containing amino acids 1–205 of human Bcl-2 (1:100; Santa Cruz Biochemicals); (*b*) rabbit anti–mouse Bcl-x (see above; 1:500); (*c*) two different preparations of affinity-purified rabbit antibodies raised against amino acids 43–61 of the mouse Bax (see above; 1:500); (*d*) mouse mAbs to Bak that react with the orthologous mouse and human proteins (Calbiochem, La Jolla, CA; 1:100); (*e*) affinity-purified c-Raf antibodies (see above; 1:500); (*f*) rabbit anti–mouse pRB (Santa Cruz Biochemicals; 1:500); (*g*) rabbit anti–mouse cyclin D1 (Upstate Biotechnology, Inc., Lake Placid, NY; 1:100); (*h*) anti–mouse cdk4 (see above; 1:500); (*i*) rabbit anti–mouse cyclin E (Santa Cruz Biochemicals; 1:500); (*j*) anti–mouse cdk2 (see above; 1:500); (*k*) goat anti–BrdU sera (Cohn and Lieberman, 1984; 1:1,000); (*l*) mouse mAb against subunit I of human cytochrome oxidase (5D4-F5; Molecular Probes, Eugene, OR; 1:100); and (*m*) rabbit anti–SV-40 TAg (obtained from Doug Hanahan, University of California, San Francisco, CA; 1:1,000). Formalin-fixed tissues were used to identify Bcl-2, Bax, Bak, Bcl-x, c-Raf-1, pRB, cyclin D1, cdk4, cdk2, and cytochrome oxidase subunit I. BrdU and cyclin E expression were surveyed in Bouin's-fixed tissues.

Antigen–antibody complexes were detected using indocarbocyanine (Cy3)-labeled donkey anti–rabbit Ig (Jackson ImmunoResearch, West Grove, PA; 1:500), FITC-labeled donkey anti–goat Ig (Jackson ImmunoResearch; 1:100); Cy3-sheep anti–mouse Ig (Jackson ImmunoResearch; 1:500), or FluorX-conjugated donkey anti–mouse IgG (Biological Detec-

tion Systems, Amersham Life Sciences, Arlington, IL; 1:200). Nuclei were stained with bis-benzimide (Sigma Chemical Co.; 0.05 μg/ml PBS). Blocking controls were performed by preincubating the primary antibodies with their peptide antigens overnight at 4°C before application to tissue sections.

Immunohistochemical Analysis of the Crypt–Villus Pattern of Expression of Integrins and Their Ligands Using Tyramide Signal Amplification

The spatial distribution of these proteins was examined in P42–60 normal and transgenic mice (*n* = 2–4 animals/group) using the following panel of antibodies: (*a*) rat anti–mouse β_1 integrin mAb (clone 9EG7; PharMingen, San Diego, CA; diluted 1:2,000); (*b*) rabbit anti–mouse α_3 integrin (Chemicon, Temecula, CA; 1:4,000); (*c*) rabbit anti–mouse α_5 integrin (Chemicon; 1:2,000); (*d*) rat anti–human/mouse α_6 mAb (clone GoH3, PharMingen; 1:4,000) (*e*) rat anti–mouse β_4 mAb (clone 346-11A; PharMingen; 1:2,000); (*f*) rabbit anti–mouse fibronectin (Chemicon; 1:5,000); (*g*) rabbit anti–mouse laminin (recognizes both A and B laminin isoforms; Chemicon; 1:5,000); and (*h*) rabbit anti–mouse type IV collagen (Chemicon; 1:5,000).

Mice were sacrificed, and the middle third of the small bowel was flushed with PBS and then frozen in OCT (Miles, Inc., Kanakee, IL). Serial 5-μm-thick sections were cut, fixed in methanol (−20°C for 15 min), washed three times (3 min/cycle) in PBS, and treated with PBS-blocking buffer for 15 min at room temperature. Cells with endogenous peroxidase activity were labeled by incubating the frozen sections for 10 min at room temperature with FITC-conjugated biotinyl-tyramide (New England Nuclear Life Sciences, Boston, MA; diluted 1:100 in 1× amplification diluent from the same manufacturer). After three washes in PBS (5 min each), the sections were incubated overnight at 4°C with one of the primary antibodies listed above and then washed in TNT buffer (0.1 M Tris, pH 7.5/0.15 M NaCl/0.05% Tween-20; 3 cycles; 5 min each). HRP-conjugated goat anti–rat or goat anti–rabbit Ig were added (Kirkegaard and Perry Labs, Gaithersburg, MD; diluted 1:100 in TNB buffer [0.1 M Tris, pH 7.5/0.15M NaCl/0.5% blocking reagent from New England Nuclear Life Sciences]). After a 30-min incubation at room temperature, sections were washed three times with TNT buffer (5 min each). Biotinyl-tyramide was added (diluted 1:100 in 1× amplification diluent) for 10 min. Sections were washed three times in TNT buffer (5 min/cycle), subsequently overlaid with Cy3-conjugated streptavidin (New England Nuclear Life Sciences; diluted 1:500 in TNB) for 30 min, and then subjected to three more rinses in TNT buffer before coverslips were added.

Two controls were performed for each experiment using a given primary antiserum: direct amplification of endogenous peroxidase activity alone (see above) and omission of primary antibodies.

Quantitation of Apoptosis

Terminal deoxynucleotidyltransferase (TdT)–mediated, dUTP nick end labeling (TUNEL) assays were performed on sections of formalin-fixed Swiss rolls using the protocol of Gavrieli et al. (1992), except that sections were incubated with proteinase K (Boehringer Mannheim Corp.; 20 μg/ml) for 20 min at 23°C. Incorporation of digoxigenin-labeled dUTP was detected using peroxidase-conjugated sheep anti–digoxigenin Fab fragments (Boehringer Mannheim Corp.; diluted 1:500 in PBS-blocking buffer) and the Vector VIP kit (Vector Laboratories, Burlingame, CA). Sections were counterstained in methyl green (Zymed Labs, S. San Francisco, CA).

The number of TUNEL-positive epithelial cells with apoptotic morphology (Wyllie et al., 1980, Hall et al., 1994) were scored in a blinded fashion by two observers. All intact crypt–villus units present in two nonadjacent sections of a Swiss roll prepared from the distal half of the small intestine were surveyed (*n* = 3–5 animals/genotype). Statistical analyses were performed using Student's *t* test (SigmaPlot; Jandel Corp., San Rafael, CA).

Quantitation of the Ratio of S-phase to M-phase Cells

The small intestine was removed from single transgene-containing and bitransgenic mice that had been pulse-labeled 90 min before sacrifice with BrdU. Jejunal segments were fixed in Bouin's, embedded in paraffin, and serial 5-μm sections were stained with hematoxylin and eosin or with antibodies to BrdU. M-phase and S-phase cells in crypts and villi were
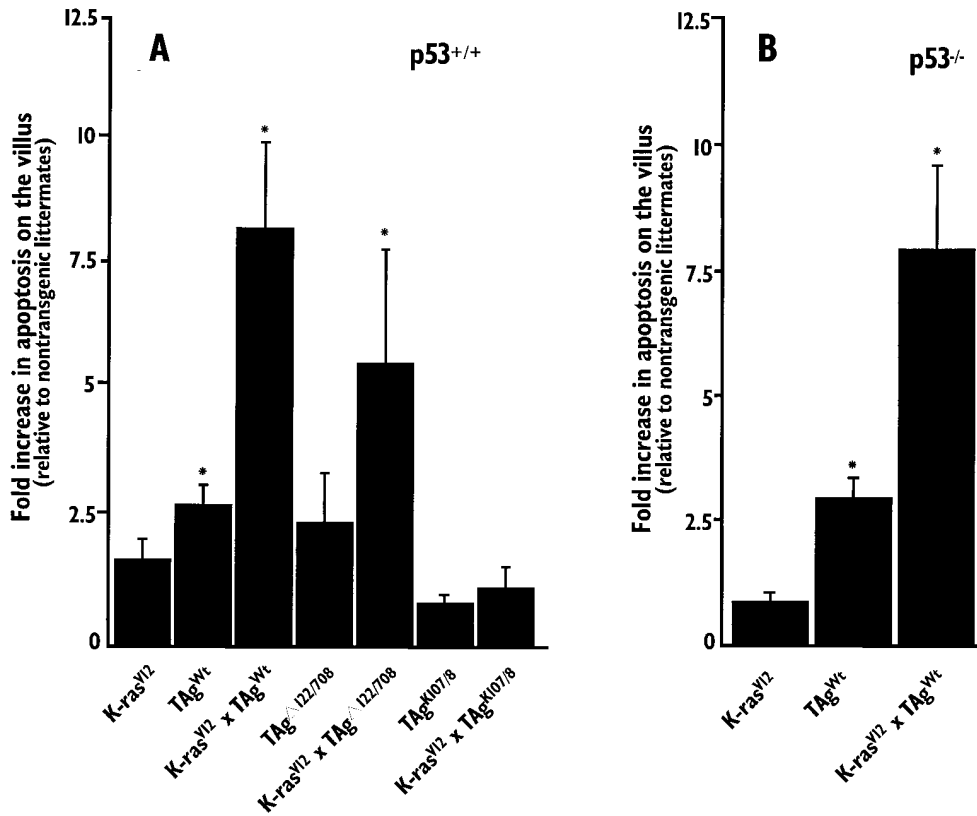
Figure 1. Quantitative analysis of apoptosis in the jejunal villus epithelium of adult transgenic and bi-transgenic mice homozygous for p53 wild-type or null alleles. (*A*) Postnatal day (P) 42 $p53^{+/+}$ FVB/N transgenic mice. (*B*) P42 $p53^{-/-}$ animals with equivalent genetic backgrounds. An asterisk indicates that the results obtained for animals of this genotype are significantly different from normal littermate controls ($P < 0.05$). Crypt apoptosis was not significantly different between normal nontransgenic animals and any of the single transgene-containing or bi-transgenic mice (data not shown).

counted in adjacent serial sections. 40 well-oriented crypt–villus units were scored per section ($n = 2$ sections/mouse; 3 mice/genotype).

Measurements of K-ras^{Val12} mRNA Levels

Total cellular RNA was isolated from the jejunum of single transgene-containing animals, bi-transgenic mice, and normal littermates. K-ras^{Val12} mRNA levels were defined using a ribonuclease protection assay (Kim et al., 1993). The 199 base cRNA yields a 148 base protected fragment when annealed to the mRNA product of *Fabpi*–K-ras^{Val12} and a 54 base protected fragment when annealed to the mRNA product of the endogenous mouse c-K-ras^{Gly12} gene.

Results

Studies of Bi-transgenic Mice Indicate That K-ras^{Val12} Augments the p53-independent Apoptosis Produced by SV-40 TAg^{Wt} in Villus Enterocytes

We examined the effect of an activated Ras, human K-ras^{Val12}, on apoptosis in villus enterocytes of transgenic mice. K-ras^{Val12} was selected because it is the most common activated Ras found in intestinal neoplasms (Bos et al., 1987; Forrester et al., 1987).

Studies in transgenic mice have shown that nucleotides -1178 to $+28$ of the rat intestinal fatty acid binding protein gene (*Fabpi*) can be used to restrict expression of foreign gene products to postmitotic villus enterocytes distributed along the length of the small intestine (e.g., Cohn et al., 1992; Kim et al., 1993; Hermiston et al., 1996). Transgene expression is activated just as enterocytes emerge from the crypt and is sustained as they complete their upward migration to the villus' apical extrusion zone. *Fabpi*–reporter transgenes are first expressed coincident with the initial cytodifferentiation of the intestinal epithelium on embryonic day 15. Expression is maintained for at least the first 2 yr of life.

Ribonuclease protection assays indicated that like other *Fabpi*$^{-1178 \text{ to } +28}$-containing transgenes, *Fabpi*–K-ras^{Val12} is expressed at highest levels in the middle third of the small intestine (jejunum) of 6–8-wk-old FVB/N mice (data not shown).

Quantitative TUNEL and morphologic assays of apoptosis in P42–60 *Fabpi*–K-ras^{Val12} transgenic mice and their normal littermates revealed that production of K-ras^{Val12}

Figure 2. Expression of cdk2 in FVB/N normal, transgenic, and bi-transgenic mice. (*A*) Western blot of jejunal protein extracts (75 μg/lane) prepared from P42 mice, probed with affinity-purified antibodies to cdk2. Lane *1*, nontransgenic FVB/N mouse; lane *2*, *Fabpi*–K-ras^{Val12} animal; lane *3*, *Fabpi*–SV-40 TAg^{Wt} mouse; lane *4*, K-ras^{Val12} × SV-40 TAg^{Wt} bi-transgenic animal; lane *5*, K-ras^{Val12} × SV-40 TAg$^{K107/8}$ bi-transgenic mouse. (*B–D*) Expression of cdk2 along jejunal crypt–villus units of a P42 normal FVB/N mouse (*B*), a *Fabpi*–SV-40 TAg^{Wt} transgenic littermate (*C*), and a P42 K-ras^{Val12} × SV-40 TAg^{Wt} bi-transgenic mouse (*D*). Cdk2 was detected by incubating the tissue sections with the same rabbit anti–mouse cdk2 preparation used for the Western blotting experiment shown in *A* and Cy3-conjugated donkey anti–rabbit Ig. Cdk2 (*red*) is confined to proliferating crypt epithelial cells in the normal FVB/N mouse. (The closed arrows in *B* point to a crypt–villus junction; the open arrow points to a crypt base columnar epithelial cell. These cells represent prolifer-

170
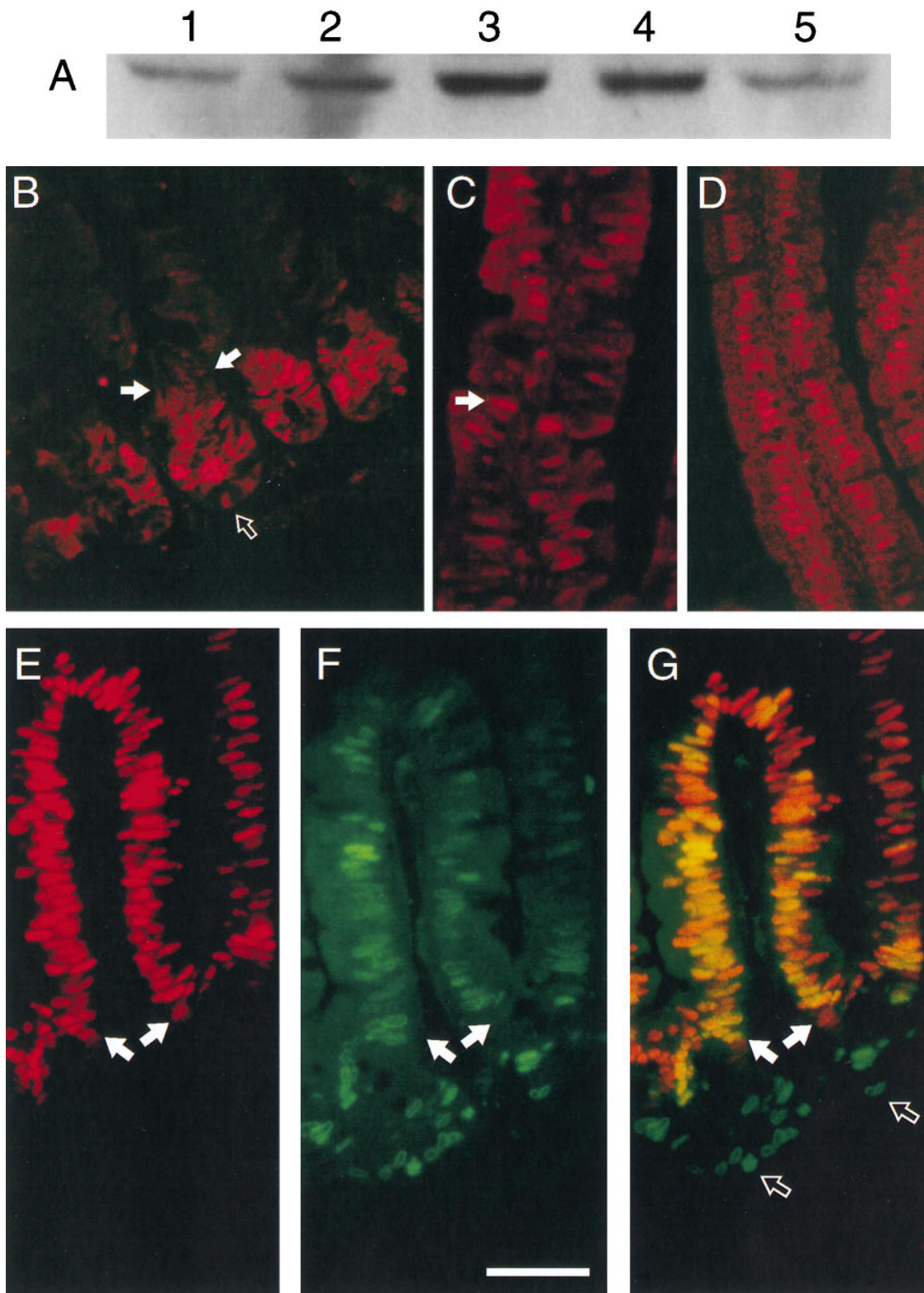
ating precursors of the enterocytic lineage and are intermixed with differentiated Paneth cells at the base of crypts [Cheng and Leblond, 1974a].) SV-40 TAg^Wt expression is associated with an induction of cdk2 in villus enterocytes (e.g., *C, arrow*). A similar induction of cdk2 in villus enterocytes is evident in the bi-transgenic animal (*D*). (*E–G*) Multilabel immunohistochemical study of a jejunal crypt–villus unit from the bi-transgenic mouse shown in *D*, establishing that villus enterocytes have reentered the cell cycle. The mouse received an intraperitoneal injection of BrdU 1.5 h before sacrifice. The section was stained with rabbit anti–SV-40 TAg (visualized in *E* with Cy3-donkey anti–rabbit Ig) and goat anti-BrdU (visualized in *F* with FITC-conjugated donkey anti–goat Ig). *G* is a dual exposure of the section confirming that BrdU-positive cells distributed along the length of the villus also express SV-40 TAg^Wt (*yellow-orange staining nuclei*). The closed arrows in *E–G* indicate the location of the crypt–villus junction. The open arrows in *G* point to proliferating crypt epithelial cells that do not express SV-40 TAg^Wt. (*Fabpi*–directed expression of SV-40 TAg^Wt is limited to villus enterocytes.) Bar, 25 µm.

in jejunal villus enterocytes produces no statistically significant change in their basal level of apoptosis (Fig. 1 *A*). This is true whether animals are $p53^{+/+}$ or $p53^{-/-}$ (Fig. 1, *A* and *B*). Apoptotic cells are limited to the tips of villi in both *Fabpi*–K-ras^{Val12} animals and their nontransgenic FVB/N cagemates.

Forced expression of K-ras^{Val12} has no detectable effect on the pattern of accumulation of regulators of the G1/S transition of the cell cycle. Terminal differentiation of normal FVB/N enterocytes is associated with rapid loss of cyclin D1 and cdk2 but not their partners, cdk4 and cyclin E. Cellular levels of pRB do not change as enterocytes move from the base to the tips of villi, although pRB phosphorylation appears to diminish (Chandrasekaran et al., 1996). Immunohistochemical and Western blot analyses of normal and transgenic mouse intestine revealed that K-ras^{Val12} does not affect expression of these cell cycle regulators (Fig. 2 *A*, plus data not shown), nor does it cause villus enterocytes to reenter the cell cycle, whether judged by their ability to incorporate BrdU or by the appearance of M-phase cells (data not shown).

Other markers of terminal differentiation of the enterocytic lineage, including a complex pattern of glycoconjugate production defined by in situ binding of members of a panel of lectins to fixed sections of intestine (Falk et al., 1994; Hermiston and Gordon, 1995), are unaffected by K-ras^{Val12} (data not shown).

Fabpi-directed expression of SV-40 TAg^{Wt} in villus enterocytes induces cyclin D1 and cdk2 expression and causes cell cycle reentry (Chandrasekaran et al., 1996). SV-40 TAg^{Wt}-induced reentry is accompanied by a statistically significant threefold increase in villus epithelial cell apoptosis ($P < 0.05$; Fig. 1 *A*). Apoptotic cells are present in the lower and mid-portion of *Fabpi*–SV-40 TAg^{Wt} villi, regions where apoptotic events are undetectable in normal FVB/N littermates (data not shown).

Crossing FVB/N *Fabpi*–K-ras^{Val12} mice to FVB/N *Fabpi*–SV-40 TAg^{Wt} mice yields bi-transgenic animals with a proliferating and dysplastic population of enterocytes. The dysplasia is manifested in part by branched villi (Fig. 3 *A*). K-ras^{Val12} augments the apoptosis observed in SV-40 TAg^{Wt}–positive villus enterocytes; bi-transgenic mice have a statistically significant threefold increase in apoptotic cells in jejunal villi compared to *Fabpi*–SV-40 TAg^{Wt} transgenics, and a statistically significant six- to ninefold increase when compared to mice containing *Fabpi*–K-ras^{Val12} alone or no transgenes (Fig. 1 *A*). Apoptotic cells are evident in the lower and middle thirds of villi and occur in regions with and without dysplasia (Fig. 3, *A–D*).

The augmented apoptosis in bi-transgenic mice cannot be attributed to alterations in K-ras^{Val12} or SV-40 TAg expression. Ribonuclease protection assays indicated that K-ras^{Val12} mRNA levels are equivalent in jejunal RNAs isolated from animals containing *Fabpi*–K-ras^{Val12} alone or *Fabpi*–K-ras^{Val12} and *Fabpi*–SV-40 TAg^{Wt}. SV-40 TAg^{Wt} mRNA levels are also indistinguishable in *Fabpi*–SV-40 TAg^{Wt} transgenic and K-ras^{Val12} × SV-40 TAg^{Wt} bi-transgenic animals (data not shown).

The steady-state levels plus intracellular and crypt–villus distributions of pRB, cyclin D1, cyclin E, cdk4, and cdk2 are the same in *Fabpi*–SV-40 TAg^{Wt} and K-ras^{Val12} × SV-40 TAg^{Wt} animals. In addition, there is no statistically

significant difference in the ratio of S-phase to M-phase cells in the jejunal villi of bi-transgenic K-ras^{Val12} × SV-40 TAg^{Wt} mice compared to their *Fabpi*–SV-40 TAg^{Wt} littermates (Fig. 2, *A–G*, plus data not shown). These results indicate that the K-ras^{Val12} effect on apoptosis is not due to increases in either proliferation or abortive cell cycle reentry.

K-ras^{Val12} Can Only Augment Apoptosis When SV-40 TAg Is Able to Produce Cell Cycle Reentry

SV-40 TAg$^{K107/8}$ is a mutant with Lys for Glu substitutions at residues 107 and 108. These substitutions block the ability of TAg to bind pRB and the related pocket proteins p107 and p130 but do affect p53 binding (Fanning and Knippers, 1992). (p107 and p130 are not detectable in the small intestinal epithelium of adult FVB/N mice using commercially available antibodies and a variety of sensitive immunohistochemical detection methods [Chandrasekaran et al., 1996].) We analyzed adult (6–8-wk-old) FVB/N *Fabpi*–SV-40 TAg$^{K107/8}$ transgenic mice with equivalent concentrations of TAg in their total jejunal protein extracts as our *Fabpi*–SV-40 TAg^{Wt} animals (Chandrasekaran et al., 1996). Expression of the mutant TAg in villus enterocytes does not induce cyclin D1 or cdk2, does not cause reentry into the cell cycle, and does not cause any significant increase in apoptosis compared to normal littermate controls (Fig. 1 *A*, plus data not shown). Coexpression of K-ras^{Val12} and SV-40 TAg$^{K107/8}$ in bi-transgenic mice does not change the growth-arrested state of villus enterocytes, as judged by their lack of incorporation of BrdU, by the lack of cells in M-phase, and by the lack of detectable changes in the steady-state levels or crypt–villus distributions of pRB, cyclins D1 and E, and their partners cdk4 and cdk2 (e.g., compare lanes *1* and *5* in Fig. 2 *A*). There are no dysplastic changes in the small intestinal epithelium of these animals ($n = 15$). Moreover, K-ras^{Val12} × SV-40 TAg$^{K107/8}$ mice do not manifest any significant increases in villus apoptosis when compared to nontransgenic FVB/N animals or FVB/N mice containing either one of the transgenes alone (Fig. 1 *A*).

p53 Is Not Required

A comparison of the phenotypes of K-ras^{Val12} × SV-40 TAg$^{K107/8}$ and K-ras^{Val12} × SV-40 TAg^{Wt} mice establishes a linkage between pRB and the observed apoptotic response of villus enterocytes. It also indicates that functional domains of the viral oncoprotein, other than its pRB binding region, are not sufficient to induce death in villus enterocytes or to mediate the further enhancement of apoptosis by K-ras^{Val12}. An analysis of cell death in the jejunal crypt–villus units of 6–8-wk-old $p53^{+/+}$ and $p53^{-/-}$ K-ras^{Val12} × SV-40 TAg^{Wt} mice provided definitive proof that K-ras^{Val12} augments apoptosis through a p53-independent pathway (Fig. 1, *A* and *B*).

The Presence or Absence of Dysplasia Has Little Effect on the Ability of K-ras to Increase Apoptosis in Cycling Villus Enterocytes

SV-40 TAg$^{\Delta122 \text{ to } 708}$ is a truncation mutant that contains the NH$_2$-terminal 121 residues of the viral oncoprotein. It retains the ability to bind pRB and related pocket proteins
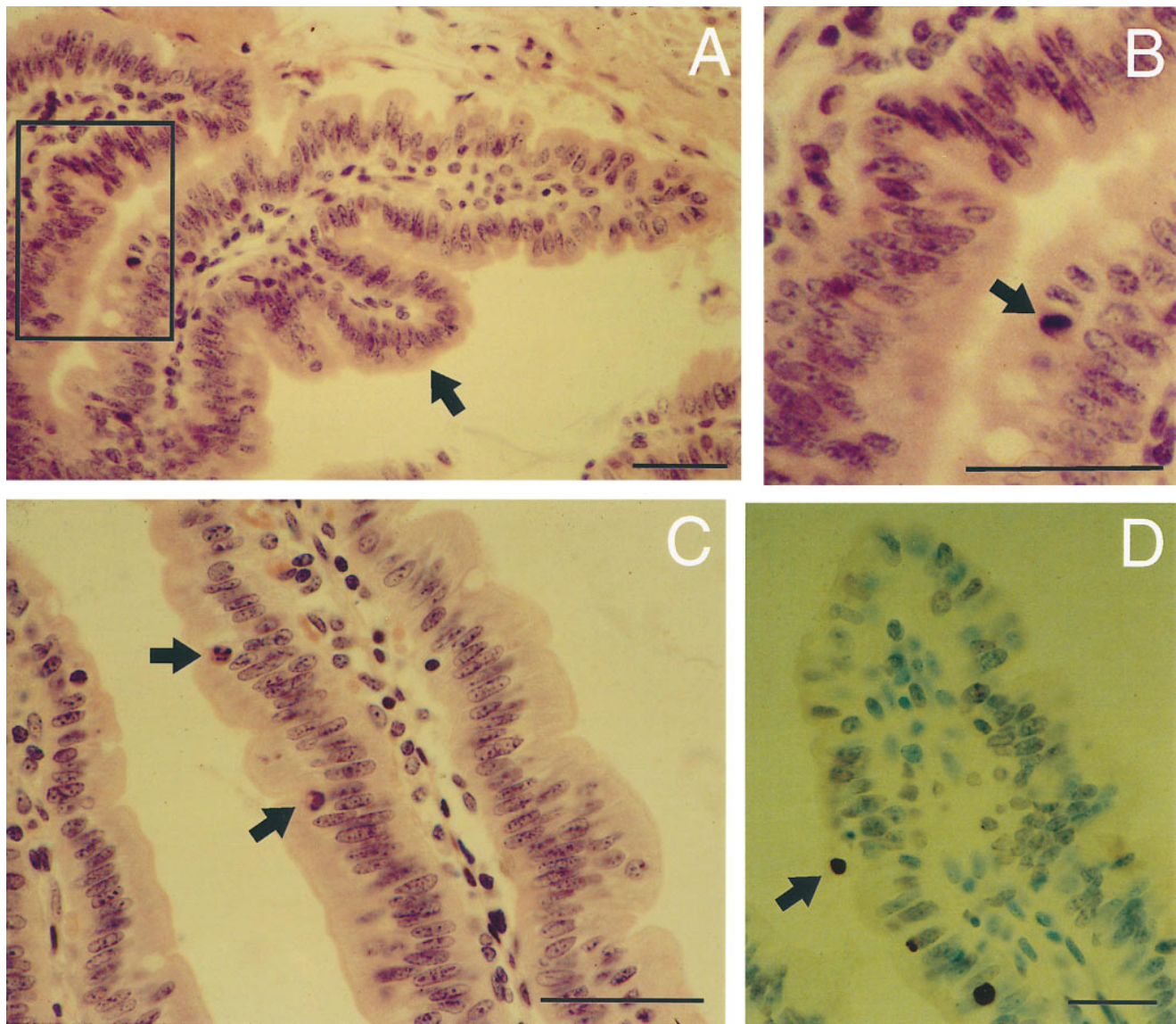
Figure 3. Distribution of apoptotic cells in jejunal villi of a P42 K-ras^{Val12} × SV-40 TAg^{Wt} bi-transgenic animal. (*A*) Villus section stained with hematoxylin and eosin. The arrow points to a branch. Such branching is not seen in normal villi. (*B*) High power view of the boxed region in *A*. The closed arrow points to an apoptotic cell. (*C* and *D*) Apoptotic cells, whether defined by histologic criteria (*C*, *arrows*) or by the TUNEL assay (e.g., *D*, *arrow*), are numerous and distributed in the middle (as well as lower and upper) third of villi. Bars, 25 μm.

but does not interact with p53 (Srinivasan et al., 1989). We examined members of a pedigree of FVB/N *Fabpi*–SV-40 TAg$^{\Delta122\ to\ 708}$ mice whose jejunal TAg levels were equivalent to those observed in FVB/N *Fabpi*–SV-40 TAg^{Wt} and *Fabpi*–SV-40 TAg$^{K107/8}$ animals. Cdk2 is induced in the villus enterocytes of *Fabpi*–SV-40 TAg$^{\Delta122\ to\ 708}$ mice. Reentry into the cell cycle occurs, although the proliferative response is less than what is observed with SV-40 TAg^{Wt} (e.g., the steady-state concentrations of cdk2 in jejunal protein extracts are 50–60% of those in age-matched *Fabpi*–SV-40 TAg^{Wt} animals; $n = 3$ mice/genotype). Coexpression of K-ras^{Val12} and the truncation mutant does not produce dysplasia in jejunal villi (Kim et al., 1994). Nonetheless, coexpression results in a statistically significant ($P < 0.05$) 2.3-fold increase in apoptosis compared to age-matched *Fabpi*–SV-40 TAg$^{\Delta122\ to\ 708}$ cagemates (Fig. 1 *A*).

Coexpression of K-ras^{Val12} and SV-40 TAg^{Wt} Has No Appreciable Effect on the Crypt–Villus Distribution or Steady-State Levels of Bcl-2, Bcl-x$_L$, Bak, Bax, and c-Raf-1

Previous studies of the effect of Ras oncoproteins on apoptosis in a variety of cultured cell lines implicated Bcl-2 and/or p53 as mediators (Fernandez-Sarabia and Bischoff, 1993; Tanaka et al., 1994; Chen and Faller, 1995, 1996; Kinoshita et al., 1995; Lin et al., 1995; Wang et al., 1995). Therefore, the distribution of several regulators of apoptosis were analyzed along the jejunal crypt–villus units of normal FVB/N mice and in littermates containing all combinations of the transgenes described above. Bak (bcl-2 homologous antagonist/killer) is proapoptotic (Chittenden et al., 1995; Farrow et al., 1995; Kiefer et al., 1995). Bcl-2 is

an antiapoptotic (Bakhshi et al., 1985; Cleary and Sklar, 1985; Tsujimoto et al., 1985). Alternative splicing of the *Bcl-x* gene gives rise to Bcl-x_L, which is antiapoptotic, and Bcl-x_S, which is proapoptotic (Boise et al., 1993; N.B. Western blots indicate that Bcl-x_L represents >95% of total jejunal Bcl-x in normal and bi-transgenic animals; data not shown).

Differentiation of the enterocytic lineage is normally associated with an upregulation of Bcl-2 and Bcl-x_L without appreciable expression of Bak. The increased apoptosis seen along the length of SV-40 TAg^{Wt}, K-ras^{Val12} × SV-40 TAg^{Wt}, and K-ras^{Val12} × SV-40 TAg$^{\Delta122 \text{ to } 708}$ jejunal villi is not associated with any remarkable change in the cellular or intracellular patterns of accumulation of these proteins.
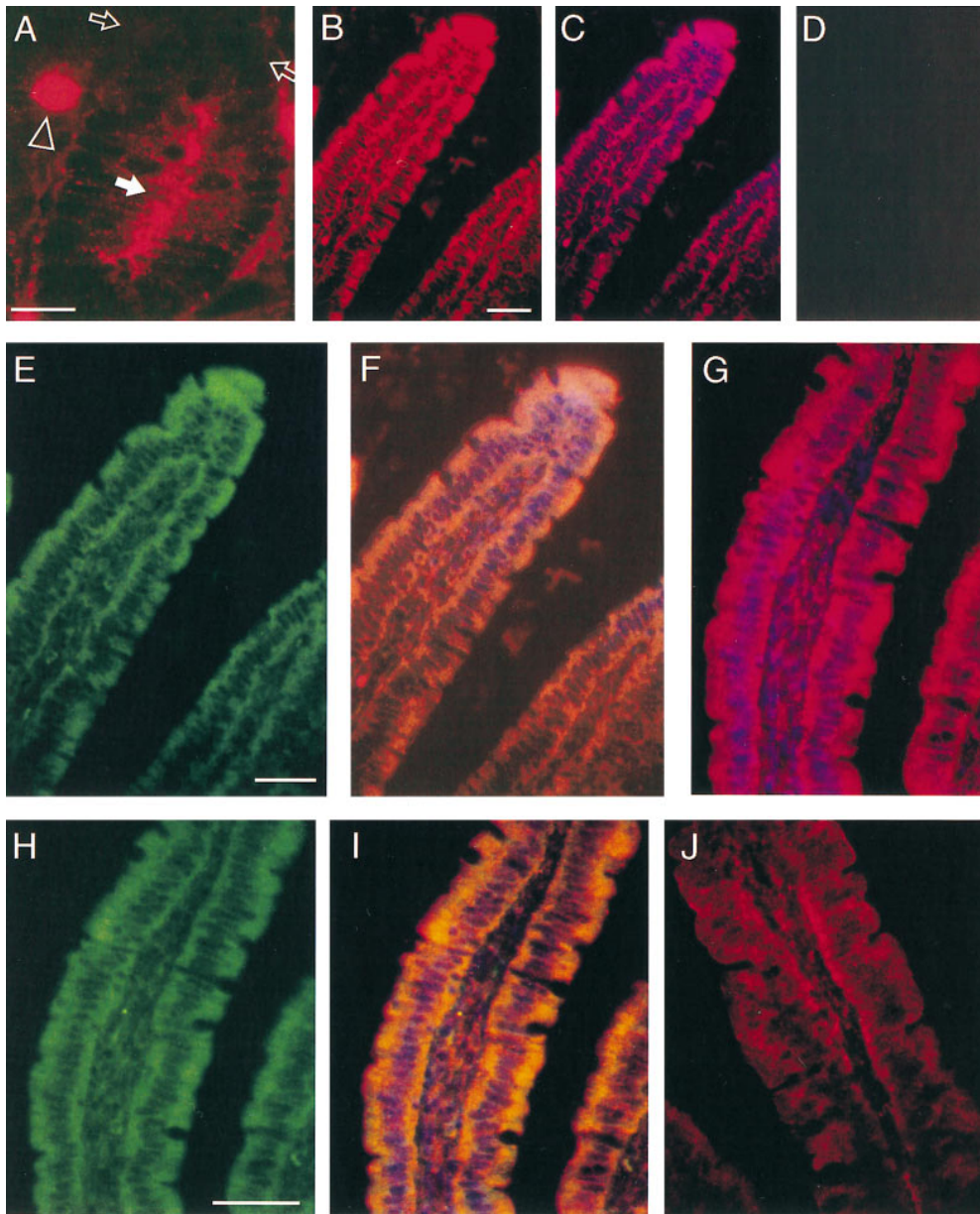

Figure 4. Cellular and intracellular distributions of Bak, Bcl-2, Bcl-x_L, and c-Raf-1 in jejunal crypt–villus units of P42 bi-transgenic K-ras^{Val12} × SV-40 TAg^{Wt} mice. (*A*) Section of a crypt stained with mouse monoclonal antibodies to Bak and Cy3-sheep anti–mouse Ig. The open arrows point to a crypt–villus junction. The apical surfaces of crypt epithelial cells are intensely stained (*closed arrow*). Bak falls to undetectable levels as postmitotic enterocytes emerge from the crypt and enter the lower quarter of the villus. The open arrowhead points to one of several lamina propria lymphocytes that react with secondary Cy3-conjugated sheep antibodies to mouse Ig. (*B–F*) Distribution of the antiapoptotic mediator Bcl-2. (*B*) Section of a bi-transgenic jejunal villus stained with affinity-purified rabbit anti–Bcl-2 plus Cy3-donkey anti–rabbit Ig. (*C*) Same section stained as in *B* but with a nuclear stain (bis-benzimide; *blue*). (*D*) Blocking control in which the primary antibody was incubated with the peptide antigen from which it was generated, before application to another jejunal crypt–villus unit. (*E*) Same section as shown in *B* and *C*, stained with mouse mAbs against cytochrome oxidase subunit I, a mitochondrial protein, and FluorX-conjugated donkey anti–mouse Ig. (*F*) A triple exposure of *C* and *E*. Bcl-2 is barely detectable in the central portion of crypts where the proliferating transit cell population resides or at the crypt base were Paneth cells are located (data not shown). Cellular levels rise markedly just as enterocytes exit the crypt. There is no appreciable change in steady-state concentration or intracellular distribution of Bcl-2 as enterocytes complete their migration up the villus. The distribution of Bcl-2 within enterocytes is similar to the distribution of the mitochondrial marker, consistent with its previously described organelle affiliation in other cell lineages (Hockenbery et al., 1990). (*G–I*) Antibodies to Bcl-x produce a crypt–villus and intracellular pattern of staining that mimics that of Bcl-2. *G* is a section of a bi-transgenic jejunal villus incubated with affinity-purified rabbit anti–Bcl-x, Cy3-donkey anti–rabbit Ig, and bis-benzimide. *H* shows the same section stained with mouse mAbs to subunit I of cytochrome oxidase and FluorX-conjugated donkey anti–mouse Ig. *I* is a triple exposure. (*J*) Jejunal villus from a bi-transgenic mouse stained with affinity-purified rabbit anti–c-Raf-1 and Cy3-donkey anti–rabbit Ig. c-Raf is expressed in epithelial cells distributed throughout the length of jejunal crypt–villus units. Cellular levels do not change appreciably as cells complete their migration-associated terminal differentiation. Immunoreactive protein is absent from the nucleus and present throughout the cytoplasm, where it produces a granular pattern of staining. Bars, 25 µm.

Bak remains confined to the crypt and is not induced in cycling villus enterocytes (Fig. 4 *A*). Bcl-2 remains undetectable or barely detectable in crypt epithelial cells, continues to be induced at the crypt–villus junction, and is not suppressed as cells move to the villus tip, even though they are dividing (Fig. 4, *B–I*). The crypt–villus and intracellular distributions of Bcl-x$_L$ are similar to those of Bcl-2 in all cases (e.g., compare *G–I* with *C, E,* and *F* in Fig. 4). Western blots of jejunal extracts prepared from transgenic and bi-transgenic mice established that expression of K-ras^{Val12}, SV-40 TAg^{Wt}, SV-40 TAg$^{K107/8}$, or SV-40 TAg$^{\Delta122\ to\ 708}$ alone, or K-ras^{Val12} plus the various SV-40 TAgs, has no appreciable effects on the steady state levels of Bcl-2, Bcl-x$_L$, or the proapoptotic mediator Bax (Oltvai et al., 1993) (Fig. 5).[2]

Recent studies of cultured cells suggest that c-Raf-1, a serine-threonine kinase that plays a central role in the mitogen-activated kinase signaling pathway, may also operate downstream of Ras and upstream of Bcl-2 to promote death (Wang et al., 1994; Blagosklonny et al., 1996). Coexpression of K-ras^{Val12} and SV-40 TAg^{Wt} does not perturb the cellular patterns of c-Raf-1 accumulation (Fig. 4 *J*) or the steady-state level of this protein (Fig. 5).

Expression of SV-40 TAg^{Wt} and K-ras^{Val12} Does Not Have a Detectable Affect on the Crypt–Villus Patterns of Accumulation of Integrins or Their Ligands

Depending upon the cell type, interactions with extracellular matrix (ECM) can either promote anchorage-dependent growth or signal cell cycle arrest and terminal differentiation (Lin and Bissell, 1993). Anoikis refers to the propensity of cultured (epithelial or endothelial) cells to undergo apoptosis when dissociated from extracellular matrix (Meredith et al., 1993; Frisch and Francis, 1994; for review see Ruoslahti and Reed, 1994). Integrins have been implicated as mediators of these responses to the ECM (Meredith et al., 1993; Boudreau et al., 1995; Zhang et al., 1995; Pullan et al., 1996; Wary et al., 1996; Frisch et al., 1996). A Ras-linked MAP kinase pathway has been identified recently that functions to reduce the affinity of some integrins for their ligands (Hughes et al., 1997).

It is possible that cycling SV-40 TAg^{Wt}–positive villus enterocytes or dysplastic K-ras^{Val12} × SV-40 TAg^{Wt} enterocytes have altered interactions with the ECM and that such alterations curtail their survival; after all, apoptosis is

---

2. Three different preparations of Bax antibodies, two raised against a peptide spanning residues 43–61 of the protein and the other against residues 11–30, yielded the expected patterns of reactivity with jejunal, spleen, and thymic proteins prepared from mice homozygous for wild-type or null alleles of Bax; a 21-kD protein was detected in Bax$^{+/+}$ tissue extracts but was absent from Bax$^{-/-}$ extracts. Affinity-purified polyclonal antibodies against residues 11–30 failed to detect Bax in sections of jejunal crypt–villus units prepared from Bax$^{+/+}$ or Bax$^{-/-}$ animals. However, both preparations of antibodies to residues 43–61 produced similar patterns of staining in Bax$^{-/-}$ and Bax$^{+/+}$ animals, whether jejunal sections were fixed in Bouin's solution or formalin and whether or not antigen unmasking protocols were used. In all cases, staining was blocked by preincubation of the antibody with the Bax peptide before its application to tissue sections. Immunoreactive Bax, or what is presumed to be a protein with a shared epitope, is present at low levels in epithelial cells distributed from the base to the tip of villi. The protein(s) are undetectable in the upper and middle thirds of the crypt. However, long-lived Paneth cells located at the crypt base are intensely stained (data not shown).
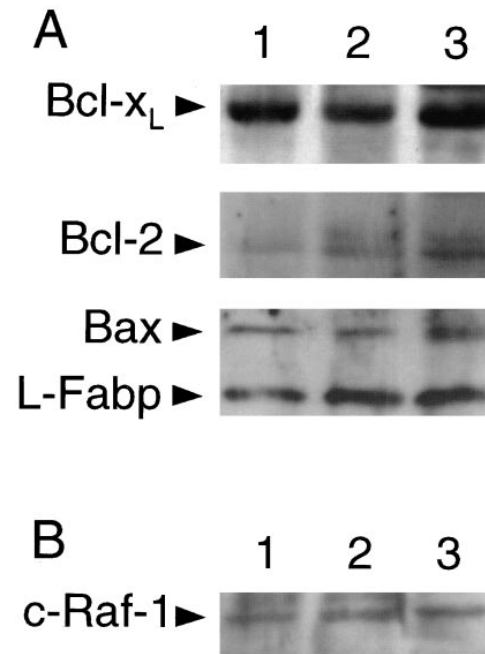

Figure 5. Western blot analysis of the steady-state levels of Bcl-2, Bcl-x$_L$, Bax, and c-Raf-1 in jejunal extracts prepared from P42 FVB/N normal, transgenic, and bi-transgenic animals. Total jejunal proteins (75 μg/lane) were fractionated by SDS-PAGE. Replicate protein blots were probed with antibodies to regulators of apoptosis or liver fatty acid–binding protein (L-Fabp; an enterocytic marker). (*A*) Lane *1*, extract from a *Fabpi*–K-ras^{Val12} mouse; lane *2*, extract from a *Fabpi*–SV-40 TAg^{Wt} mouse; lane *3*, extract from a bi-transgenic K-ras^{Val12} × SV-40 TAg^{Wt} animal. (*B*) Lane *1*, normal FVB/N mouse; lane *2*, *Fabpi*–SV-40 TAg^{Wt} animal; lane *3*, bi-transgenic K-ras^{Val12} × SV-40 TAg^{Wt} mouse. The results shown are representative of those obtained with three to eight animals/genotype.

normally limited to the same apical region of the villus where cells detach from the matrix (and from one another) and are exfoliated into the lumen (Hall et al., 1994). Therefore, we used sensitive immunohistochemical detection methods (i.e., tyramide signal amplification; Bobrow et al., 1989; Shindler and Roth, 1996) to analyze the effects of expressing K-ras^{Val12}, SV-40 TAg^{Wt}, or both oncoproteins on the crypt–villus distributions of integrins associated with the regulation of epithelial cell growth and survival ($\alpha_5\beta_1$) and with intestinal epithelial cell adhesion to the ECM ($\alpha_6\beta_4$) (Giancotti and Ruoslahti, 1990; Mortarini et al., 1992; Ruoslahti and Reed, 1994; Simon-Assmann et al., 1994; Zhang et al., 1995).

In normal FVB/N mice, α_5, α_6, β_1, and β_4 integrin subunits accumulate at the base of all epithelial cells in crypt–villus units (Fig. 6, *A, E, H, L,* and *M*). α_3, another β_1 partner, is limited to the basal surface of villus epithelial cells (data not shown). These patterns are not perturbed in *Fabpi*–K-ras^{Val12} or *Fabpi*–SV-40 TAg^{Wt} animals or in their bi-transgenic littermates (*n* = 2–4 animals/genotype; Fig. 6, *A–O*).

VLA5 ($\alpha_5\beta_1$) and VLA3 ($\alpha_3\beta_1$) function as receptors for fibronectin. In nontransgenic FVB/N mice, fibronectin is distributed in the ECM from the crypt base to the villus tip (Fig. 6 *P*). Expression of K-ras^{Val12} or SV-40 TAg^{Wt}, alone
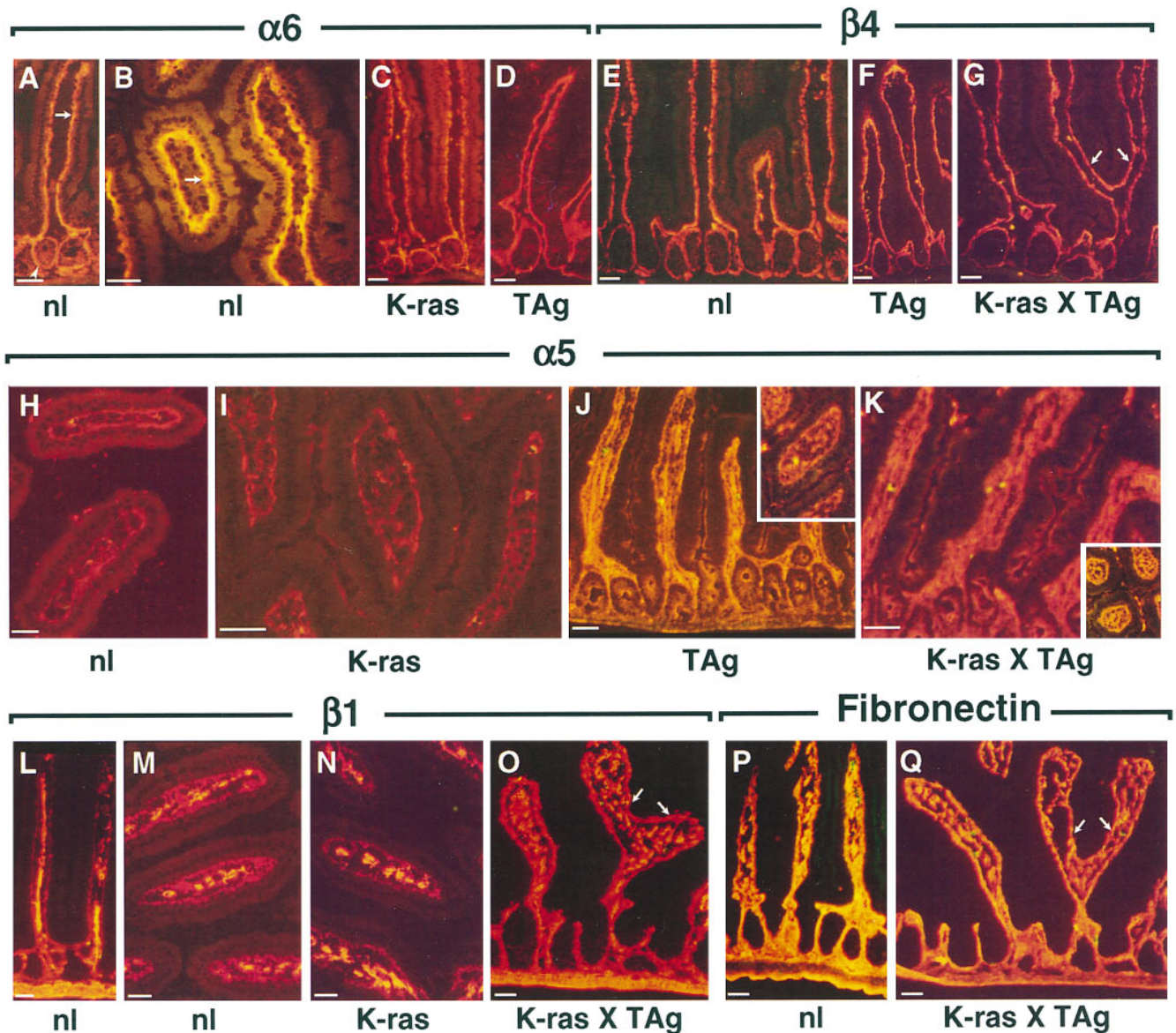
Figure 6. Immunohistochemical analysis of the crypt–villus pattern of accumulation of integrin subunits and their ligands in 6-wk-old FVB/N normal, transgenic, and bi-transgenic mice. Frozen sections of jejunum were processed as described in Materials and Methods. The top of each panel is labeled to show the protein that is being examined. The bottom of each panel gives the genotype of the mouse. Antigen–antibody complexes were detected using HRP-conjugated secondary antibodies, biotinyl tyramide amplification, and Cy3-streptavidin. Integrin subunits and integrin ligands appear red-orange. Cells that contain endogenous peroxidase activity were colabeled with FITC–biotinyl tyramide and Cy3-streptavidin and appear yellow-green. *nl*, normal (nontransgenic) FVB/N mouse; *K-ras*, littermate containing the *Fabpi*–K-ras^{Val12} transgene; *TAg*, *Fabpi*–SV-40 TAg^{Wt} transgenic animal; *K-ras × TAg*, *Fabpi*–K-ras^{Val12} × *Fabpi*–SV-40 TAg^{Wt} bi-transgenic mouse. (*A*) The α_6 integrin subunit is evident at the basal surfaces of epithelial cells distributed from the base of the crypt (*closed arrowhead*) through the length of the villus (e.g., *closed arrow*). (*B*) Higher power view of a normal villus sectioned at its midpoint, perpendicular to the crypt–villus axis. The arrow points to immunoreactive α_6 at the base of enterocytes. (*C* and *D*) The crypt–villus distribution of α_6 is similar in transgenic mice and does not differ from the distribution observed in their normal littermate shown in *A* and *B*. (*E–G*) The β_4 subunit integrin is present throughout crypt–villus units in normal, *Fabpi*–SV-40 TAg^{Wt} transgenic, and bi-transgenic animals. The arrows in *G* point to a branched (bifurcated) villus. Branching is one manifestation of the dysplasia observed in the small intestine of bi-transgenic mice. (*H–K*) Distribution of α_5 integrin subunit. *H* and *I* show jejunal villi that have been sectioned at their midpoint, perpendicular to the crypt–villus axis. Immunoreactive protein is present at the base of villus enterocytes and in cellular components of the lamina propria. *J* and *K* show sections cut parallel to the crypt–villus axis. The insets in each of these two panels show cross sections taken at the midpoint of *Fabpi*–SV-40 TAg^{Wt} and bi-transgenic jejunal villi. The integrin subunit is distributed from the base to the villus tip in all animals (*J* and *K* plus data not shown). (*L–O*) The β_1 subunit follows the distribution of its α_5 partner. *L* and *M* show normal jejunal villi sectioned parallel and perpendicular to the crypt–villus axis, respectively. *N* illustrates results obtained from cross sections of *Fabpi*–K-ras^{Val12} villi. *O* contains a branched villus (*arrows*) from a bi-transgenic animal. (*P* and *Q*) Fibronectin shows a similar distribution along the crypt–villus axis of normal and bi-transgenic mice, as that of its receptor, $\alpha_5\beta_1$ integrin. Bars, 25 μm.

or in combination, has no detectable effect on the accumulation of fibronectin (Fig. 6, *P* and *Q*) or on the crypt–villus distribution of two other integrin ligands present in the ECM: type IV collagen and laminin (data not shown).

Interactions between epithelial cells can also affect their susceptibility to anoikis and survival (Frisch and Francis, 1994). E-cadherin is the principal epithelial cadherin in the adult mouse small intestine and is present at the adherens junctions and basolateral surfaces of all villus enterocytes. Forced expression of a dominant negative N-cadherin mutant in jejunal villus enterocytes results in a loss of E-cadherin from the cell surface, a marked reduction in cellular pools of E-cadherin, disruption of cell–cell as well as cell–substratum contacts, and precocious entry into a death program (Hermiston and Gordon, 1995). In light of this previous finding, immunohistochemical surveys were conducted with a well-characterized mouse E-cadherin monoclonal antibody (Hermiston and Gordon, 1995). The results indicated that expression of K-ras^{Val12} and/or SV-40 TAg^{Wt} has no appreciable effects on the intracellular or crypt–villus distributions of E-cadherin ($n = 2$–5 mice/genotype; data not shown).

Discussion

We have used transgenic mice containing various combinations of K-ras^{Val12} plus wild-type or mutant SV-40 TAgs to show that K-ras^{Val12} augments the apoptosis that accompanies a pRB-related reentry of differentiated small intestinal enterocytes into the cell cycle.

The augmented apoptosis occurs through an as yet unknown mechanism. It does not require p53. It is not accompanied by detectable changes in accumulation of regulators of the G1/S transition (pRB, cyclins D1 and E, cdks 2 and 4) or enhanced proliferation. It is not associated with changes in the crypt–villus patterns of expression of several regulators of apoptosis (Bcl-2, Bcl-x$_L$, Bak, Bax, and c-Raf-1). The enhancement is not accompanied by changes in the crypt–villus distribution of mediators of epithelial cell–matrix and cell–cell interactions and survival (e.g., $\alpha_5\beta_1$ integrin and its ligand fibronectin or E-cadherin). In some cases our assays may be too insensitive to rule out involvement. For example, an inability to detect alterations in the crypt–villus pattern of accumulation of five integrin subunits (α_3, α_5, α_6, β_1, and β_4) or E-cadherin does not definitively prove that attachment of enterocytes to the ECM or to adjacent cells is unperturbed in bi-transgenic animals, or that integrin-activated intracellular signaling events that affect survival (e.g., Frisch et al., 1996; Wary et al., 1996) are fully functional. A recent study using CHO cells indicated that H-ras and its effector kinase, Raf-1, function to negatively regulate the ligand binding affinity of certain integrins (Hughes et al., 1997). Such a finding is consistent with the notion that an anoikis-like mechanism may contribute to the increased apoptosis seen in bi-transgenic mice.

Because K-ras^{Val12} is the most commonly mutated oncogene in colorectal cancer, our in vivo results have implications concerning the multistep journey to intestinal neoplasia. As in primary cultures of human and rodent cells, villus enterocytes are not transformed through forced expression of K-ras^{Val12}. The known collaboration that occurs in primary cell cultures between activated forms of Ras and pRB-disabling viral oncoproteins such as E1A, E7, or SV-40 TAg^{Wt} also applies to enterocytes. Bi-transgenic K-ras^{Val12} × SV-40 TAg^{Wt} mice exhibit dysplasia in their villus epithelium by the time that crypt–villus morphogenesis is completed between P21–28. This dysplasia is manifested in part by branched villi. Branching involves the epithelium, its underlying ECM, and the lamina propria (e.g., Fig. 6, *G*, *O*, and *Q*), providing an interesting model system for examining how the small intestinal epithelium is able to define overall villus structure.

Despite the early onset of this dysplasia, bi-transgenic animals do not develop small intestinal neoplasms between 2 and 18 mo of age ($n = 40$ animals). The lack of progression may be due to the increased apoptosis produced by K-ras^{Val12} in this "initiated" cell population with a proliferative abnormality. Another contributing factor may be the short residence time of migrating enterocytes on the villus; without functional anchorage, they are not able to undergo clonal expansion. As noted in the introduction, K-ras^{Val12} is the most commonly mutated oncogene in human colorectal tumors (Fearon and Vogelstein, 1990). Activating K-ras mutations are not acquired at the beginning but rather at intermediate points in the multistep journey to intestinal neoplasia (Bos et al., 1987; Forrester et al., 1987; Fearon and Vogelstein, 1990). Our results are consistent with this observation. K-ras^{Val12} alone has no detectable effect on noncycling enterocytes. When expressed in "initiated" enterocytes with a proliferative abnormality, K-ras^{Val12} can facilitate progression to a dysplastic phenotype. However, by diminishing cell survival on the villus, the oncoprotein may also impede further progression.

Intestinal neoplasia is thought to be initiated in the crypt, perhaps at the level of the functionally anchored stem cell or one of its immediate daughters (Moser et al., 1992). Although the effect of K-ras^{Val12} on initiated crypt epithelial cells is unknown, our studies suggest that on the villus, K-ras^{Val12} may serve an editing function for the host, helping to remove these cells. Additional mutations may be needed to suppress the proapoptotic response to K-ras^{Val12}. Such mutations may affect genes encoding one or more determinants of cell survival. Since downregulation of apoptosis can contribute to the late stages of tumor progression, at least in model systems (Naik et al., 1996), it is tempting to speculate about the significance of the increased expression of antiapoptotic mediators, such as Bcl-x$_L$ or Bcl-2, that has been noted during progression of human colorectal tumors (Hague et al., 1994; Bedi et al., 1995; Bronner et al., 1995; Krajewska et al., 1996). Crossing bi-transgenic K-ras^{Val12} × SV-40 TAg^{Wt} mice to mice that overexpress these or other mediators of cell survival in their gut epithelium provides one way of identifying molecules that may overcome the K-ras^{Val12}-augmented apoptosis and thus promote development of gut neoplasia.

References

Bakhshi, A., J.P. Jensen, P. Goldman, J.J. Wright, O.W. McBride, A.L. Epstein, and S.J. Korsmeyer. 1985. Cloning the chromosomal breakpoint of t(14;18) human lymphomas: clustering around J_H on chromosome 14 and near a transcriptional unit on 18. *Cell.* 41:899–906.

Barbacid, M. 1987. Ras genes. *Ann. Rev. Biochem.* 56:779–827.

Bedi, A., P.J. Pasricha, A.J. Akhtar, J.P. Barber, G.C. Bedi, F.M. Giardiello, B.A. Zehnbauer, S.R. Hamilton, and R.J. Jones. 1995. Inhibition of apoptosis during development of colorectal cancer. *Cancer Res.* 55:1811–1816.

Blagosklonny, M.V., T. Schulte, P. Nguyen, J. Trepel, and L.M. Neckers. 1996. Taxol-induced apoptosis and phosphorylation of Bcl-2 protein involves c-Raf-1 and represents a novel c-Raf-1 signal transduction pathway. *Cancer Res.* 56:1851–1854.

Bobrow, M.N., T.D. Harris, K.J. Shaughnessy, and G.J. Litt. 1989. Catalyzed reporter deposition, a novel method of signal amplification. *J. Immunol. Methods.* 125:279–285.

Boise, L.H., M. Gonzalez-Garcia, C.E. Postema, L. Ding, T. Lindsten, L.A. Turka, X. Mao, G. Nunez, and C.B. Thompson. 1993. bcl-x, a bcl-2-related gene that functions as a dominant regulator of apoptotic cell death. *Cell.* 74:597–608.

Bos, J.L., E.R. Fearon, S.R. Hamilton, M. Verlaan-de Vries, J.H. van Boom, A.J. van der Eb, and B. Vogelstein. 1987. Prevalence of ras gene mutations in human colorectal cancers. *Nature (Lond.).* 327:293–297.

Boudreau, N., C.J. Sympson, Z. Werb, and M.J. Bissell. 1995. Suppression of ICE and apoptosis in mammary epithelial cells by extracellular matrix. *Science (Wash. DC).* 267:891–893.

Bronner, M.P., C. Culin, J.C. Reed, and E.E. Furth. 1995. The bcl-2 proto-oncogene and the gastrointestinal epithelial tumor progression model. *Am. J. Pathol.* 146:20–26.

Bry, L., P. Falk, K. Huttner, A. Ouellette, T. Midtvedt, and J.I. Gordon. 1994. Paneth cell differentiation in the developing intestine of normal and transgenic mice. *Proc. Natl. Acad. Sci. USA.* 91:10335–10339.

Chandrasekaran, C., C.M. Coopersmith, and J.I. Gordon. 1996. Use of normal and transgenic mice to examine the relationship between terminal differentiation of intestinal epithelial cells and accumulation of their cell cycle regulators. *J. Biol. Chem.* 271:28414–28421.

Chen, C.Y., and D.V. Faller. 1995. Direction of p21ras-generated signals towards cell growth or apoptosis is determined by protein kinase C and Bcl-2. *Oncogene.* 11:1487–1498.

Chen, C.Y., and D.V. Faller. 1996. Phosphorylation of Bcl-2 protein and association with p21Ras in Ras-induced apoptosis. *J. Biol. Chem.* 271:2376–2379.

Chen, J., G.J. Tobin, J.M. Pipas, and T. Van Dyke. 1992. T-antigen mutant activities in vivo: roles of p53 and pRB binding in tumorigenesis of the choroid plexus. *Oncogene.* 7:1167–1175.

Cheng, H. 1974a. Origin, differentiation, and renewal of the four main epithelial cell types in the mouse small intestine. II. Mucous cells. *Am. J. Anat.* 141:481–502.

Cheng, H. 1974b. Origin, differentiation, and renewal of the four main epithelial cell types in the mouse small intestine. IV. Paneth Cells. *Am. J. Anat.* 141:521–536.

Cheng, H., and C.P. LeBlond. 1974a. Origin, differentiation, and renewal of the four main epithelial cell types in the mouse small intestine. I. Columnar cells. *Am. J. Anat.* 141:461–480.

Cheng, H., and C.P. LeBlond. 1974b. Origin, differentiation, and renewal of the four main epithelial cell types in the mouse small intestine. III. Entero-endocrine cells. *Am. J. Anat.* 141:503–520.

Cheng, H., and C.P. LeBlond. 1974c. Origin, differentiation, and renewal of the four main epithelial cell types in the mouse small intestine. V. Unitarian theory of the origin of the four epithelial cell types. *Am. J. Anat.* 141:537–561.

Chittenden, T., E.A. Harrington, R. O'Connor, C. Flemington, R.J. Lutz, G.I. Evan, and B.C. Guild. 1995. Induction of apoptosis by the Bcl-2 homologue Bak. *Nature (Lond.).* 374:733–736.

Cleary, M.L., and J. Sklar. 1985. Nucleotide sequence of a t(14;18) chromosomal breakpoint in follicular lymphoma and demonstration of a breakpoint-cluster region near a transcriptionally active locus on chromosome 18. *Proc. Natl. Acad. Sci. USA.* 82:7439–7443.

Cohn, S.M., and M.W. Lieberman. 1984. The use of antibodies to 5-bromo-2′-deoxyuridine for the isolation of DNA sequences containing excision-repair sites. *J. Biol. Chem.* 259:12456–12462.

Cohn, S.M., T.C. Simon, K.A. Roth, E.H. Birkenmeier, and J.I. Gordon. 1992. Use of transgenic mice to map cis-acting elements in the intestinal fatty acid binding protein gene (*Fabpi*) that control its cell lineage-specific and regional patterns of expression along the duodenal-colonic and crypt-villus axes of the gut epithelium. *J. Cell Biol.* 119:27–44.

Falk, P., K.A. Roth, and J.I. Gordon. 1994. Lectins are sensitive tools for defining differentiation programs of mouse gut epithelial cell lineages. *Am. J. Physiol. (Gastrointest. Liver Physiol.)* 266:G987–G1003.

Fanning, E., and R. Knippers. 1992. Structure and function of simian virus 40 large tumor antigen. *Ann. Rev. Biochem.* 61:55–85.

Farrow, S.N., J.H.M. White, I. Martinou, T. Raven, K.-T. Pun, C.J. Grinham, J.-C. Martinou, and R. Brown. 1995. Cloning of a bcl-2 homologue by interaction with adenovirus E1B 19K. *Nature (Lond.).* 374:731–733.

Fearon, E.R., and B. Vogelstein. 1990. A genetic model for colorectal tumorigenesis. *Cell.* 61:759–767.

Fernandez, A., M.C. Marin, T. McDonnell, and H.N. Ananthaswamy. 1994. Differential sensitivity of normal and Ha-ras-transformed C3H mouse embryo fibroblasts to tumor necrosis factor: induction of bcl-2, c-myc, and manganese superoxide dismutase in resistant cells. *Oncogene.* 9:2009–2017.

Fernandez-Sarabia, M.J., and J.R. Bischoff. 1993. Bcl-2 associates with the ras-related protein R-ras p23. *Nature (Lond.).* 366:274–275.

Forrester, K., C. Almoguera, K. Han, W.E. Grizzle, and M. Perucho. 1987. Detection of high incidence of K-ras oncogenes during human colon tumorigenesis. *Nature (Lond.).* 327:298–303.

Frisch, S.M., and H. Francis. 1994. Disruption of epithelial cell–matrix interactions induces apoptosis. *J. Cell Biol.* 124:619–626.

Frisch, S.M., K. Vuori, E. Ruoslahti, and P.-Y. Chan-Hui. 1996. Control of adhesion-dependent cell survival by focal adhesion kinase. *J. Cell Biol.* 134:793–799.

Gavrieli, Y., Y. Sherman, and S.A. Ben-Sasson. 1992. Identification of programmed cell death in situ via specific labeling of nuclear DNA fragmentation. *J. Cell Biol.* 119:493–501.

Giancotti, F.G., and E. Ruoslahti. 1990. Elevated levels of the $\alpha_5\beta_1$ fibronectin receptor suppress the transformed phenotype of Chinese hamster ovary cells. *Cell.* 60:849–859.

Hague, A., M. Moorghen, D. Hicks, M. Chapman, and C. Paraskeva. 1994. Bcl-2 expression in human colorectal adenomas and carcinomas. *Oncogene.* 9:3367–3370.

Hall, P.A., P.J. Coates, B. Ansari, and D. Hopwood. 1994. Regulation of cell number in the mammalian gastrointestinal tract: the importance of apoptosis. *J. Cell Sci.* 107:3569–3577.

Hermiston, M.L., and J.I. Gordon. 1995. In vivo analysis of cadherin function in the mouse small intestinal epithelium: essential role in adhesion, maintenance of differentiation, and regulation of programmed cell death. *J. Cell Biol.* 129:489–506.

Hermiston, M.L., M.H. Wong, and J.I. Gordon. 1996. Forced expression of E-cadherin in the mouse intestinal epithelium slows cell migration and provides evidence for non-autonomous regulation of cell fate in a self-renewing system. *Genes Dev.* 10:985–996.

Hirama, T., and H.P. Koeffler. 1995. Role of the cyclin-dependent kinase inhibitors in the development of cancer. *Blood.* 86:841–854.

Hockenbery, D., G. Nunez, C. Milliman, R.D. Schreiber, and S.J. Korsmeyer. 1990. Bcl-2 is an inner mitochondrial membrane protein that blocks programmed cell death. *Nature (Lond.).* 348:334–336.

Hollstein, M., K. Rice, M.S. Greenblatt, T. Soussi, R. Fuchs, T. Sorlie, E. Hovig, B. Smith-Sorensen, R. Montesano, and C.C. Harris. 1994. Database of p53 gene somatic mutations in human tumors and cell lines. *Nucleic Acids Res.* 22:3551–3555.

Hughes, P.E., M.W. Renshaw, M. Pfaff, J. Forsyth, V.M. Keivens, M.A. Schwartz, and M.H. Ginsberg. 1997. Suppression of integrin activation: a novel function of a Ras/Raf-initiated MAP kinase pathway. *Cell.* 88:521–530.

Kiefer, M.C., M.J. Brauer, V.C. Powers, J.J. Wu, S.R. Umansky, L.D. Tomei, and P.J. Barr. 1995. Modulation of apoptosis by the widely distributed Bcl-2 homologue Bak. *Nature (Lond.).* 374:736–739.

Kim, S.H., K.A. Roth, A.R. Moser, and J.I. Gordon. 1993. Transgenic mouse models that explore the multistep hypothesis of intestinal neoplasia. *J. Cell Biol.* 123:877–893.

Kim, S.H., K.A. Roth, C.M. Coopersmith, J.M. Pipas, and J.I. Gordon. 1994. Expression of wild-type and mutant simian virus 40 large tumor antigens in villus-associated enterocytes of transgenic mice. *Proc. Natl. Acad. Sci. USA.* 91:6914–6918.

Kinoshita, T., T. Yokota, K. Arai, and A. Miyajima. 1995. Regulation of Bcl-2 expression by oncogenic Ras protein in hematopoietic cells. *Oncogene.* 10:2207–2212.

Knudson, C.M., K.S.K. Tung, W.G. Tourtellotte, G.A.J. Brown, and S.J. Korsmeyer. 1995. Bax-deficient mice with lymphoid hyperplasia and male germ cell death. *Science (Wash. DC).* 270:96–99.

Krajewska, M., S.F. Moss, S. Krajewski, K. Song, P.R. Holt, and J.C. Reed. 1996. Elevated expression of Bcl-x and reduced bak in primary colorectal adenocarcinomas. *Cancer Res.* 56:2422–2427.

Laemmli, U.K. 1970. Cleavage of structural proteins during the assembly of the head of bacteriophage T4. *Nature (Lond.).* 227:680–685.

Lin, C.Q., and M.J. Bissell. 1993. Multi-faceted regulation of cell differentiation by extracellular matrix. *FASEB (Fed. Am. Soc. Exp. Biol.) J.* 7:737–743.

Lin, H.-J.L., V. Eviner, G.C. Prendergast, and E. White. 1995. Activated H-ras rescues E1A-induced apoptosis and cooperates with E1A to overcome p53-dependent growth arrest. *Mol. Cell. Biol.* 15:4536–4544.

Loeffler, M., A. Birke, D. Winton, and C. Potten. 1993. Somatic mutation, monoclonality and stochastic models of stem cell organization in the intestinal crypt. *J. Theor. Biol.* 160:471–491.

Meredith, J.E., Jr., B. Fazeli, and M.A. Schwartz. 1993. The extracellular matrix as a cell survival factor. *Mol. Biol. Cell.* 4:953–961.

Mortarini, R., A. Gismondi, A. Santoni, G. Parmiani, and A. Anichini. 1992. Role of the $\alpha_5\beta_1$ integrin receptor in the proliferative response of quiescent human melanoma cells to fibronectin. *Cancer Res.* 52:4499–4506.

Moser, A.R., W.F. Dove, K.A. Roth, and J.I. Gordon. 1992. The *Min* (multiple intestinal neoplasia) mutation: its effect on gut epithelial cell differentiation and interaction with a modifier system. *J. Cell Biol.* 116:1517–1526.

Naik, P., J. Karrim, and D. Hanahan. 1996. The rise and fall of apoptosis during multistage tumorigenesis: down-modulation contributes to tumor progres-

sion from angiogenic progenitors. *Genes Dev.* 10:2105–2116.

Newbold, R.F., and R.W. Overell. 1983. Fibroblast immortality is a prerequisite for transformation by EJ c-Ha-*ras* oncogene. *Nature (Lond.).* 304:648–651.

Oltvai, Z.N., C.L. Milliman, and S.J. Korsmeyer. 1993. Bcl-2 heterodimerizes *in vivo* with a conserved homolog, Bax, that accelerates programmed cell death. *Cell.* 74:609–619.

Pipas, J.M., K.W. Peden, and D. Nathans. 1983. Mutational analysis of simian virus 40 T antigen: isolation and characterization of mutants with deletions in the T-antigen gene. *Mol. Cell. Biol.* 3:203–213.

Pullan, S., J. Wilson, A. Metcalfe, G.M. Edwards, N. Goberdhan, J. Tilly, J.A. Hickman, C. Dive, and C.H. Streuli. 1996. Requirement of basement membrane for the suppression of programmed cell death in mammary epithelium. *J. Cell Sci.* 109:631–642.

Rak, J., Y. Mitsuhashi, V. Erdos, S. Huang, J. Filmus, and R.S. Kerbel. 1995. Massive programmed cell death in intestinal epithelial cells induced by three-dimensional growth conditions: suppression by mutant c-H-*ras* oncogene expression. *J. Cell Biol.* 131:1587–1598.

Ruoslahti, E., and J.C. Reed. 1994. Anchorage dependence, integrins, and apoptosis. *Cell.* 77:477–478.

Schmidt, G.H., M.M. Wilkinson, and B.A.J. Ponder. 1985. Cell migration pathway in the intestinal epithelium: an in situ marker system using mouse aggregation chimeras. *Cell.* 40:425–429.

Serrano, M., A.W. Lin, M.E. McCurrach, D. Beach, and S.W. Lowe. 1997. Oncogenic *ras* provokes premature cell senescence associated with accumulation of p53 and p16^{INK4a}. *Cell.* 88:593–602.

Shindler, K.S., and K.A. Roth. 1996. Double immunofluorescent staining using two unconjugated primary antisera raised in the same species. *J. Histochem. Cytochem.* 44:1331–1335.

Simon, T.C., L.J.J. Roberts, and J.I. Gordon. 1995. A 20 nucleotide element in the intestinal fatty acid binding protein gene modulates its cell lineage-specific, differentiation-dependent, and cephalocaudal patterns of expression in transgenic mice. *Proc. Natl. Acad. Sci. USA.* 92:8685–8689.

Simon, T.C., A. Cho, P. Tso, and J.I. Gordon. 1997. Suppressor and activator functions mediated by a repeated heptad sequence in the liver fatty acid binding protein gene (*Fabpl*): effects on renal, small intestinal, and colonic epithelial cell gene expression in transgenic mice. *J. Biol. Chem.* 272:10652–10663.

Simon-Assmann, P., B. Duclos, V. Orian-Rousseau, C. Arnold, C. Mathelin, E. Engvall, and M. Kedinger. 1994. Differential expression of laminin isoforms and α_6-β_4 integrin subunits in the developing human and mouse intestine. *Dev. Dyn.* 201:71–85.

Srinivasan, A., K.W. Peden, and J.M. Pipas. 1989. The large tumor antigen of simian virus 40 encodes at least two distinct transforming functions. *J. Virol.* 63:5459–5463.

Sweetser, D.A., E.H. Birkenmeier, P.C. Hoppe, D.W. McKeel, and J.I. Gordon. 1988. Mechanisms underlying generation of gradients in gene expression within the intestine: an analysis using transgenic mice containing fatty acid binding protein-human growth hormone fusion genes. *Genes Dev.* 2:1318–1332.

Tanaka, N., M. Ishihara, M. Kitagawa, H. Harada, T. Kimura, T. Matsuyama, M.S. Lamphier, S. Aizawa, T.W. Mak, and T. Taniguchi. 1994. Cellular commitment to oncogene-induced transformation or apoptosis is dependent on the transcription factor IRF-1. *Cell.* 77:829–839.

Tsujimoto, Y., J. Gorham, J. Cossman, E. Jaffe, and C.M. Croce. 1985. The t(14; 18) chromosome translocations involved in B-cell neoplasms result from mistakes in VDJ joining. *Science (Wash. DC).* 229:1390–1393.

Wang, H.-G., T. Miyashita, S. Takayama, T. Sato, T. Torigoe, S. Krajewski, S. Tanaka, L. Hovey III, J. Troppmair, U.R. Rapp, and J.C. Reed. 1994. Apoptosis regulation by interaction of Bcl-2 protein and Raf-1 kinase. *Oncogene.* 9:2751–2756.

Wang, H.-G., J.A. Millan, A.D. Cox, C.J. Der, U.R. Rapp, T. Beck, H. Zha, and J.C. Reed. 1995. R-Ras promotes apoptosis caused by growth factor deprivation via a Bcl-2 suppressible mechanism. *J. Cell Biol.* 129:1103–1114.

Wary, K.K., F. Mainiero, S.J. Isakoff, E.E. Marcantonio, and F.G. Giancotti. 1996. The adaptor protein Shc couples a class of integrins to the control of cell cycle progression. *Cell.* 87:733–743.

Weinberg, R.A. 1995. The retinoblastoma protein and cell cycle control. *Cell.* 81:323–330.

Weinberg, R.A. 1997. The cat and mouse games that genes, viruses, and cells play. *Cell.* 88:573–575.

Wyllie, A.H., J.F.R. Kerr, and A.R. Currie. 1980. Cell death: the significance of apoptosis. *Int. Rev. Cytol.* 68:251–303.

Zhang, Z., K. Vuori, J.C. Reed, and E. Ruoslahti. 1995. The $\alpha_5\beta_1$ integrin supports survival of cells on fibronectin and up-regulates Bcl-2 expression. *Proc. Natl. Acad. Sci. USA.* 92:6161–6165.